A Three-Phase Current Source Inverter with Third Harmonic Injection For Grid-Connected Renewable Power Sources

Predrag Ninković[1] , Žarko Janda[1] , Predrag Pejović[2]

[1]University of Belgrade, Nikola Tesla Institute of Electrical Engineering, Koste Glavinića 8a, 11000 Belgrade, Serbia

[2]University of Belgrade, The Department of Electronics, School of Electrical Engineering, Bulevar kralja Aleksandra 73, 11000 Belgrade, Serbia

npedja@ieent.org, janda@ieent.org, peja@etf.bg.ac.rs

Abstract: A novel three-phase voltage-synchronized current source (VSCS) converter with third harmonic injection is proposed in this paper. Compared with the conventional vector current control (VCC), phase-locked loop (PLL) is completely removed in this method. This new type of current-source inverters is suitable for application in grid-connected renewable power sources. It is based on a three-phase six-pulse inverter topology with unidirectional switches using line-synchronous control to achieve unity displacement factor at the point of common connection. An additional power circuit to implement the third-harmonic current injection technique is used in order to improve the line current total harmonic distortion. The proposed approach ensures stable operation under weak grid conditions. Experimental results on a 1.5 kW prototype with the optimal third harmonic current injection are shown. The theoretical predictions of total harmonic distortion and power factor improvement are confirmed experimentally.

Keywords: Renewable power sources, distributed power generation, voltage-synchronized current source six-pulse inverter, third-harmonic current injection, optimized third-harmonic injection

1. Introduction

The increasing global emphasis on environmental sustainability has led to a significant surge in distributed power generation systems utilizing renewable energy sources [1]. These systems are primarily integrated into the power grid via voltage-source converters (VSCs) that employ advanced

control strategies. Vector current control (VCC) has been widely adopted as a standard control method for grid-connected VSCs [2]. However, its reliance on a phase-locked loop (PLL) for grid synchronization can introduce stability issues, particularly in weak grid conditions [3]. Power synchronization control (PSC) is one alternative approach that uses the power-angle relationship for synchronization [4]. While PSC offers simplicity, it may face challenges in limiting current during fault conditions due to its inherent voltage-oriented control.

To overcome these limitations, this paper proposes a novel voltage-synchronized current source (VSCS) converter. By directly generating synchronous switching functions by processing the grid voltage, VSCS eliminates the need for a PLL and ensures robust operation in a weak grid. Furthermore, the inherent current reference generation in VSCS enables effective current limiting during disturbances. This paper delves into the theoretical foundation, implementation details, and performance evaluation of the proposed VSCS.

Lately, the number of installed small and medium size renewable power generation utilities and energy storage units grow rapidly, increasing demand for smart power electronic systems used to interface grid. Main drawback of previous solutions is a lack of support for wide operating range under different distribution network conditions, which leads to poor utilization of the facility. Using advanced power electronic systems to interface to the grid leads to significant improvement of controllability and, consequently, efficiency to a great extent. One example is grid forming inverter.

One of the very stringent requirements for grid-interfacing devices is to keep the line current undistorted or under the minimal distortion level, keeping the total harmonic distortion (THD) below few percent, according to standards. Many new topologies were proposed since the old ones could not satisfy the requests, and making the right choice has become everything but simple [5-8].

The interface converter has to provide service regardless of the generator operating conditions (high or low wind speed, insolation, etc.). This is a limiting factor when choosing a suitable power converter topology. A widely used option is to apply a boost converter for solar panels connected in series or diode bridge rectifier as a front end converter to electrical generator. In such a way a DC source of energy is provided, which is then transferred to the grid through a single- or two-step power converter. This converter is usually equipped with a kind of PWM control, what influences efficiency and reliability of the power conversion system.

In this paper, the current source inverters that apply magnetic current injection device are analyzed, and the optimal amplitude of the third harmonic injected current is determined. It is demonstrated possibility to obtain waveforms of the inverter output currents with the THD as low as 5.125%. This new type of grid connected inverter is an extension of the application of the third harmonic current injection technique, previously implemented in

rectifiers [9, 10]. Also, it is shown that the proposed inverter is suitable for application in renewable energy sources.

In Section 2, the third harmonic injection technique is revisited. Control of the proposed inverter structure is described in time domain, analyzing the inverter structure by a sequence of corresponding linear circuits in intervals lasting 60° in phase angle applying switching functions. In Section 3, optimal amplitude of the injected third harmonic current is derived, providing the minimal THD of the inverter output currents. The inverter circuit design is discussed in Section 4, while in Section 5 the control circuit is briefly outlined. Experimental results are presented in Section 6, and the conclusions are given in Section 7.

2. The Third Harmonic Current Injection Technique

It is reported in literature [9-11] that by using the third harmonic current injection technique in rectifier circuits it is possible to improve the corresponding input current harmonic distortion significantly. Also, in [9-11] the work is done in designing all the necessary circuits to upgrade standard rectifiers without changing already existing converter structure. However, the results were oriented to power consumption only, leaving the area of power generation, i.e. the inverter operating mode, uncovered.

Presented modification of the original rectifier circuit is made in order to enable reverse power flow, from DC source to AC network. The original current-sink DC load model was transformed into a controlled current source. The same applies for all current sources and current directions in the original rectifier circuit [10, 11]. In such way, the inverter topology out of the original rectifier circuit is derived, and it is shown in Fig. 1.
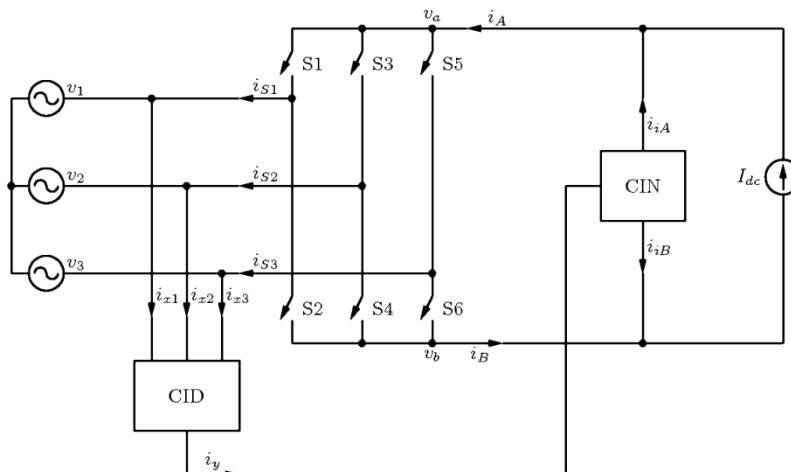

Figure 1. Structure of the inverter with the third-harmonic injection

In Fig.1, the four specific circuit parts of the main converter circuit are shown: (*i*) current source I_{dc} represents the energy source which is the appropriate type of converter connected to the input terminals, and equipped with the output current control; (*ii*) current injection network (CIN) that shapes the waveforms of the programmable currents i_{iA} and i_{iB}; (*iii*) current injection device (CID) provides the exact splitting of the current i_y into three identical currents i_{x1}, i_{x2} and i_{x3}; (*iv*) the main inverter (grid-interface converter) which is composed of six unidirectional controlled switches S1-S6. According to the third harmonic current injection technique [9, 10], it is necessary to provide a synchronized control between the main inverter switches and the current injection network in order to achieve the exact superposition of the circulating third harmonic currents and to get the sinusoidal waveform portion of the phase currents.

In order to control the main inverter, functions that determine states of the switches, named switching functions, must be derived. The phase voltages are assumed to form a three-phase symmetrical positive-sequence voltage system.

$$v_1 = V_m \cos(\omega_o t)$$
$$v_2 = V_m \cos\left(\omega_o t - \frac{2\pi}{3}\right)$$
$$v_3 = V_m \cos\left(\omega_o t + \frac{2\pi}{3}\right). \tag{1}$$

Since the basic idea of the proposed inverter solution is to force the interface converter to operate in recuperation mode with the optimal utilization, the same switching functions as in the case of the diode rectifier should be used, but in this case with unidirectional controlled switches of the opposite direction, to enable reversed current flow in comparison to the rectifier case.
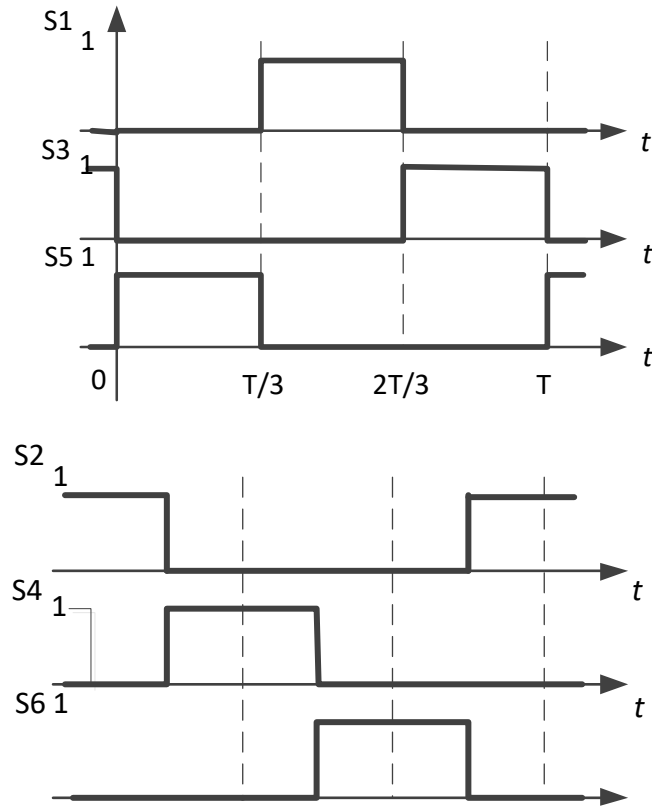
Figure 2. Switching functions of the inverter shown in Fig. 1. Positive zero crossing of voltage v_I is the zero time reference

The corresponding switching functions states are given in Figure 2, and they coincide with the three-phase diode-bridge rectifier switching functions [10]. In such a way, unity displacement power factor is achieved, which is important if generation of reactive power is not a demand. Thus, to satisfy the power factor requirements the only thing left to do is to control harmonic distortion of the line currents. As reported in [7, 8], by properly driven controlled current sources in the injection network it is possible to reduce the total harmonic distortion level significantly. To achieve this, the current sources should be controlled such that is achieved

$$i_{iA}(\omega_o t) = i_{iB}(\omega_o t) = I_{mi}\cos(3\omega_o t) \tag{2}$$

The line currents can be expressed as linear combination of products of the switching functions and currents i_A, i_B, i_{x1}, i_{x2}, and i_{x3}

$$i_1(\omega_o t) = S_1(\omega_o t)i_A(\omega_o t) - S_2(\omega_o t)i_B(\omega_o t) - i_{x1}(\omega_o t)$$
$$i_2(\omega_o t) = S_3(\omega_o t)i_A(\omega_o t) - S_4(\omega_o t)i_B(\omega_o t) - i_{x2}(\omega_o t) \qquad (3)$$
$$i_3(\omega_o t) = S_5(\omega_o t)i_A(\omega_o t) - S_6(\omega_o t)i_B(\omega_o t) - i_{x3}(\omega_o t)$$

and using inherent feature of the current injection device to split neutral point injected current i_y into three equal phase currents

$$i_{x1}(\omega_o t) = i_{x2}(\omega_o t) = i_{x3}(\omega_o t) = i_x(\omega_o t) = \frac{1}{3}i_y(\omega_o t), \qquad (4)$$

and complete set of equations which describes the circuit is

$$i_{iA}(\omega_o t) = i_{iB}(\omega_o t) = I_{mi}\cos(3\omega_o t)$$
$$i_A(\omega_o t) = I_{dc} + i_{iA}(\omega_o t)$$
$$i_B(\omega_o t) = I_{dc} - i_{iA}(\omega_o t) \qquad (5)$$
$$i_{x1}(\omega_o t) = i_{x2}(\omega_o t) = i_{x3}(\omega_o t) = i_x(\omega_o t) = \frac{2}{3}i_{iA}(\omega_o t)$$
$$i_{iA}(\omega_o t) = i_{iB}(\omega_o t) = I_{mi}\cos(3\omega_o t) \qquad .$$

In order to illustrate the principle, typical current waveforms are shown in Figs 3, 4, and 5. As it can be seen, the input current waveform is improved regarding the harmonic content as compared to the case without the third harmonic current injection.
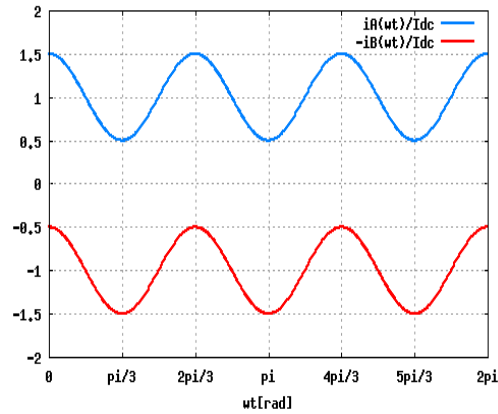

Figure 3. Waveform diagrams of DC link currents:
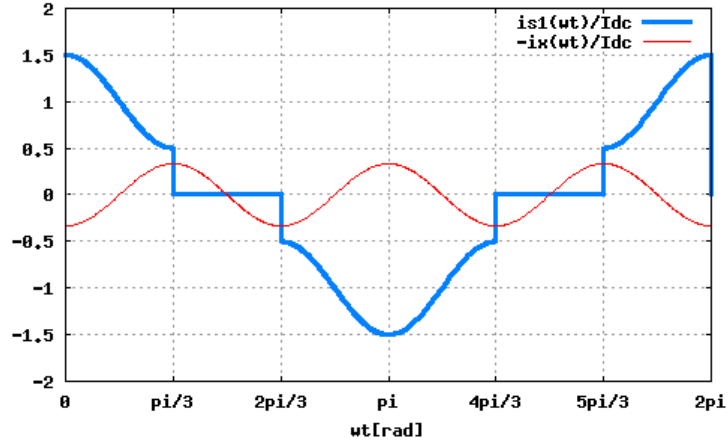upper blue trace i_A, lower red trace $-i_B$

Figure 4. Waveform diagrams of the inverter terminal current i_{s1} (thick blue trace)

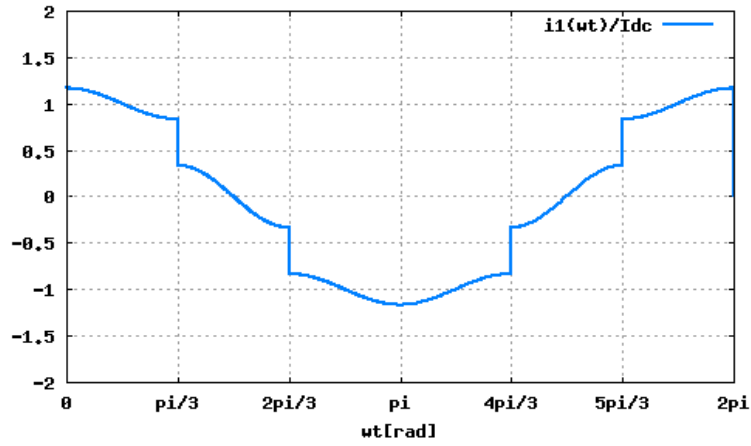*and corresponding CID current i_x (thin red trace, inversed)*

Figure 5. Waveform diagram of line current i_1.

3. The Third Harmonic Current Injection Optimization

After the system structure is chosen, the next goal is to optimize the third harmonic injected current amplitude I_{mi}, for a given input current I_{dc}, in order to minimize the output current THD. The output current RMS value expression is obtained as

$$I_{RMS}(I_{dc}, I_{mi}) = \frac{\sqrt{6I_{dc}^2 + I_{mi}^2}}{3}, \qquad (6)$$

while the corresponding fundamental harmonic amplitude is

$$I_{1,RMS}(I_{dc}, I_{mi}) = \frac{2}{\pi}\sqrt{\frac{3}{2}}I_{dc} + \frac{1}{4\pi}\sqrt{\frac{3}{2}}I_{mi}. \qquad (7)$$

Using the standard definition for THD, the value of (7) reaches its minimum for

$$I_{mi,opt} = \frac{3}{4}I_{dc}, \qquad (8)$$

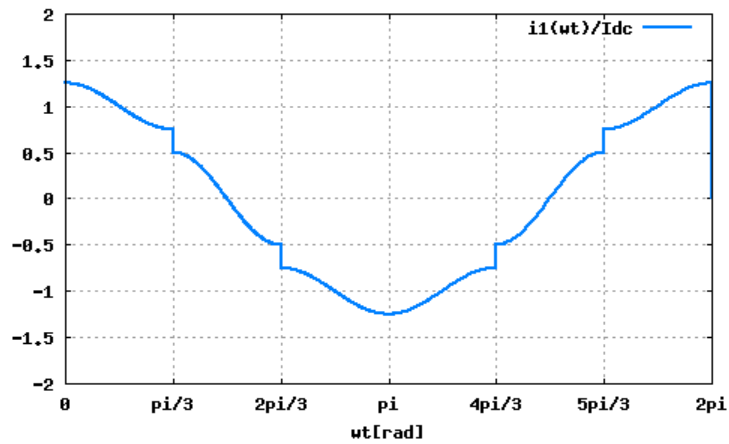resulting in $THD_{i,\min} = 5.125\%$. In that case, the line current waveform is shown in Fig. 6.

Figure 6. Line current waveform for the optimal third-harmonic injected current amplitude

4. The Experimental Circuit Design

In order to verify the proposed inverter principle, an experimental circuit is built and tested. It is based on the structure proposed in Fig. 1. To build the experimental circuit, several blocks of Fig. 1 should have been expanded to the circuit level. There are several circuits capable to substitute blocks of Fig. 1: main inverter can be realized using different devices used as unidirectional controlled switches: GTOs, IGCTs, or IGBTs in series with diodes [13]. Current injection device (CID) is usually implemented as a passive magnetic device [9, 11]. Current injection network (CIN) might be built either as a passive or an active network [9, 11]. For appropriate selection of

the circuit configurations, there are several guidelines which should be followed:

- the number of active circuits should be minimized to achieve high reliability – passive circuits should take place wherever possible;
- if an active circuit is necessary, the most reliable one, requiring the simplest control method should be used;
- optimization of the number of active components is not mandatory; maturity of the technology and the ease of operation are preferable features;
- compatibility of active components is preferable; components in different subcircuits should be the same, which leads to lower costs and shorter time-to-repair.

Based on these guidelines, a circuit shown in Fig. 7 is designed. The main inverter is made of three identical legs consisting of IGBTs with the diodes connected in series (S1-S6). This configuration results in relatively high forward voltage drop, but it can be driven by regular IGBT driver, which is a mature and reliable solution. Current-injection device is implemented as a zig-zag transformer T_{CID}, shown as a three-phase inductor in Fig. 7 for clarity.
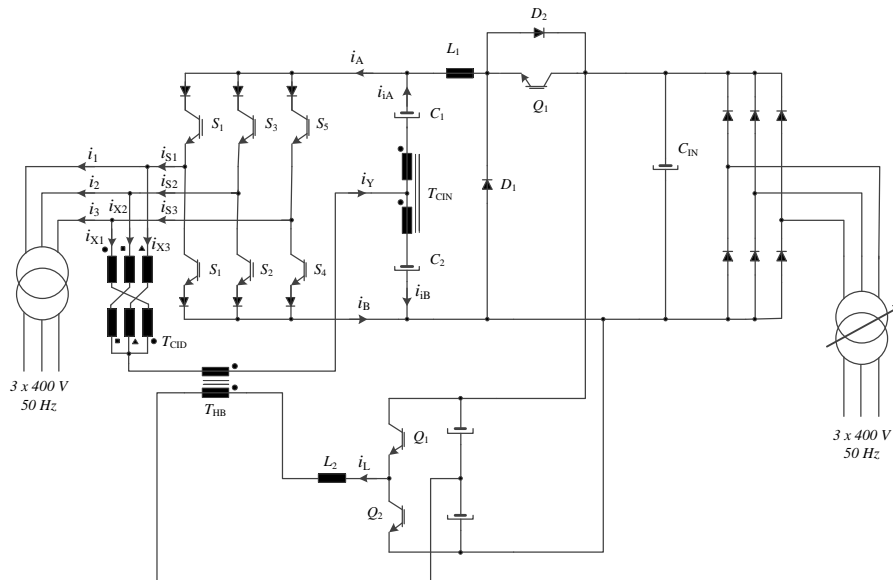

Fig. 7. The experimental circuit.

Current-source I_{dc} is realized as a buck-converter around Q_1, D_1 and L_1 where the buck inductor acts a current source for the rest of the circuit. Current-injection network is built as a hybrid network as follows:

- instead of using two different current sources, i_{iA} and i_{iB}, there is just one current source i_y and the current sharing device T_{CIN} which provides equal currents i_{iA} and i_{iB}; capacitors C_1 and C_2 suppress the DC voltage;

- current source i_y is obtained using a current controlled half-bridge inverter, supplied by the intermediate DC link; the current of inductor L_2 is controlled to achieve required waveform; transformer T_{HB} acts as a current transformer, providing appropriate amplitude of i_y and DC decoupling.

The line terminal is a standard three-phase low-voltage terminal (3x400V/50Hz). However, a set of isolating transformers is inserted in order to scale down the nominal inverter voltage to 3x231V and to achieve isolation in a case of failure (to prevent injection of the DC current into the line). Therefore, the DC voltage level of around 300V is expected to get at the DC side of the main inverter.

Variable DC voltage typical in wind generator applications is modeled by an autotransformer with a three phase diode bridge rectifier. In order to allow the buck converter to operate in continuous conduction mode, the DC voltage level should be above 350V.

5. Control Circuits

To control the proposed VSCS converter, a decentralized approach is applied, with all of the blocks having it`s own internal control structure. Since the buck converter is employed as a current source, the corresponding control block should provide tight regulation of the inductor current. Hysteretic-type control structure is chosen to control the inductor current, since the regulator is simple and robust, but suffers from variable switching frequency. The control circuit is shown in Fig. 8. Hysteresis value H defines the inductor current excursion around the average value. At the instant when the inductor current reaches the threshold level, the RS-latch circuit is triggered, and the power transistor command is toggled. The block labeled DR in Fig. 8 symbolizes the gate-driver circuit of the buck switch.
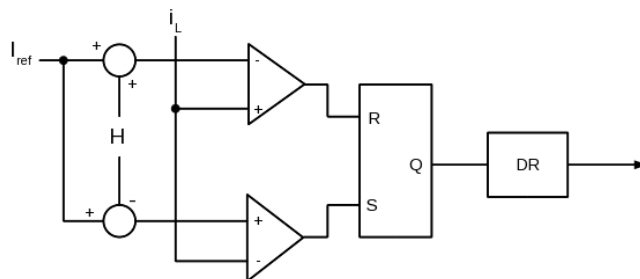

Figure 8: Buck-converter control circuit block diagram

Similar to the control of the buck converter, the half-bridge inverter control is realized applying the hysteretic-type control method. However, there are two important differences: commands for the transistors are extended

118

such that Q_1 obtains the command inverted to the command for Q_2, and the reference value greatly varies during the line cycle, being provided by some other circuit which is shown in fig 9 in the block diagram form.
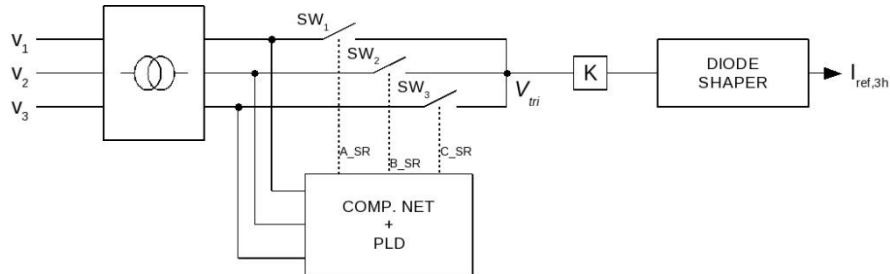

Figure 9. Obtaining reference waveform for the half-bridge injection inverter.

The circuit of Fig. 9 operates such that of analog switches SW1, SW2, and SW3 only one conducts, the one whose corresponding phase voltage is neither highest, nor the lowest among the phase voltages. At the common end of the analog switches, the voltage waveform v_{tri} is created as a sequence of phase voltages segments. This waveform contains harmonic components at triples of the line frequency [11], having triangle-like wave shape synchronized to the phase voltages. To filter out everything but the third harmonic without introducing the time shift, a nonlinear wave shaping diode circuit has to be implemented, as shown in Fig. 10. Input voltage in Figure 10 is so attenuated that the knee of diode 1N4148 exponential VA forward characteristics can be used for wave shaping. At low input voltage the diode is not conducting while at about 0.6 – 0.7 V is conducting and limiting the peak of triangular voltage waveform on a soft way, emulating sinusoidal wave shape. Gain blocks K_1 and K_2 are applied to achieve appropriate voltage gains. In such way, third harmonic reference sine wave is obtained, and it is further used as a reference signal for the half-bridge inverter output hysteretic current control
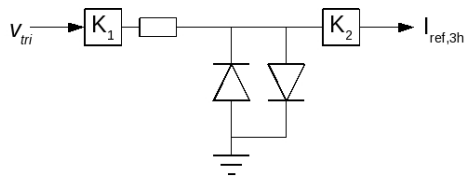

Figure 10. The waveform shaping diode circuit

Control circuitry for the main inverter is shown in Fig. 11. At a front-end, a set of voltage measuring transformers is placed, followed by the appropriate comparator network which finally forms the switching functions shown in Figure 2. Programmable logic network (PLD) is supplied by those signals, and

it generates six commands for the main inverter switches. At the output end, gate-drive circuits are connected to drive the power transistors.
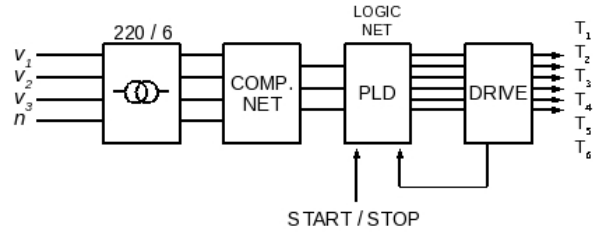

Figure 10. Block-diagram of the main inverter control circuitry

6. Experimental Results

In order to validate theoretical and simulation predictions of the proposed VSCS converter structure, the experimental setup has been built, and the main power part is shown in Figure 11.
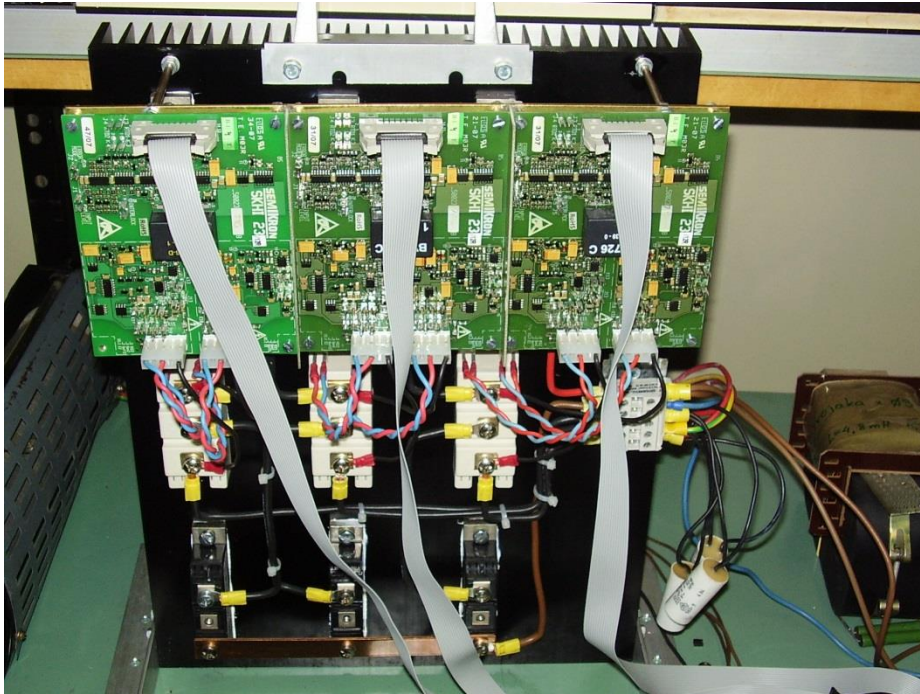

Figure 11. Power circuit of main current source inverter. Driver boards connected and RC snubbers as well are shown on the top. In bottom right corner the inductor L_1 is shown

The circuit shown in Fig. 7 is energized from both sides and the auxiliary input regulating transformer, supplying three-phase diode bridge rectifier, is set to achieve the voltage level V_{dc} of 400 V in an intermediate DC link. In the first experiment, the circuit is tested with the injection network inactive. Fig. 12 shows the line voltage and the current waveforms of the phase 1, accompanied by the corresponding THD. As expected, the phase 1 current takes pulse waveform, flowing when the phase 1 voltage is maximal or minimal, during 2/3 of the period.

In Fig. 13, three phase currents are shown in the case the current injection circuit is active. Harmonic distortions are also shown, and there is significant improvement in the current harmonic content, since the THD is decreased below 6%. The current waveforms from Fig. 13 are very similar to the waveforms shown in Fig. 6, being in agreement with the theoretical results. There is a small discrepancy between the theoretical and the experimental results, caused by the reference value for current i_y that is not a pure sinewave, being slightly distorted with THD=2.5%, and by imperfect matching of the main inverter switching matrix and the half bridge inverter reference signal. Therefore, slightly higher THD is obtained. Nevertheless, despite somewhat higher THD, the proposed injection technique is verified to be able to significantly reduce the line current THD in proposed inverters.
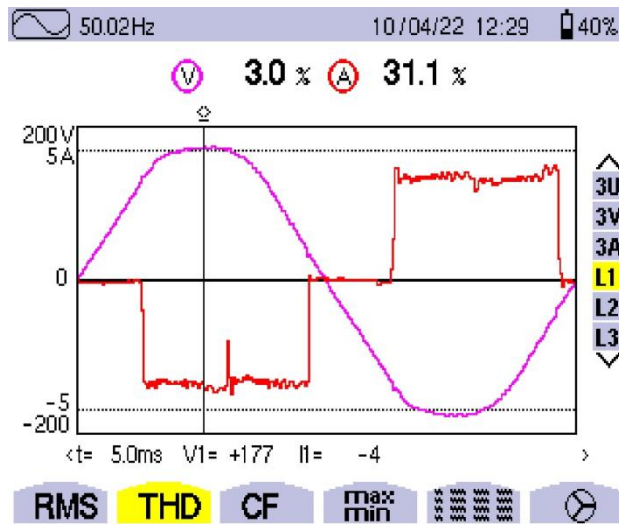

Figure 12. Phase 1 voltage and current when the injection network is disabled
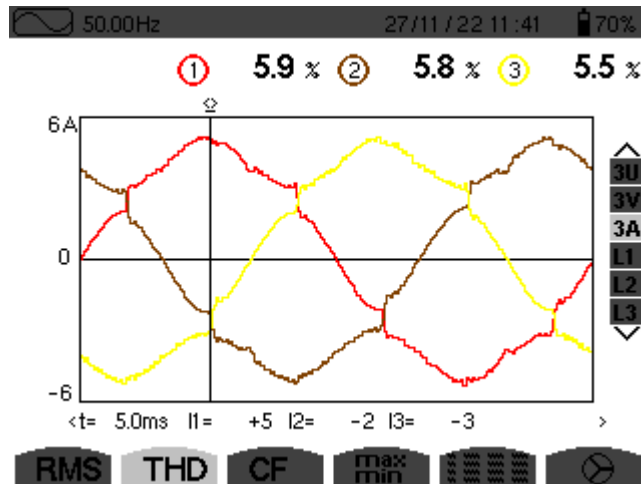
Figure 13. Line currents when the injection network is active

Fig. 14 shows phase 1 voltage and current and their corresponding THDs. There is a small displacement between the waveforms caused by slight phase-shift in main inverter switching matrix, resulting in DPF=0.997 and PF=0.994.
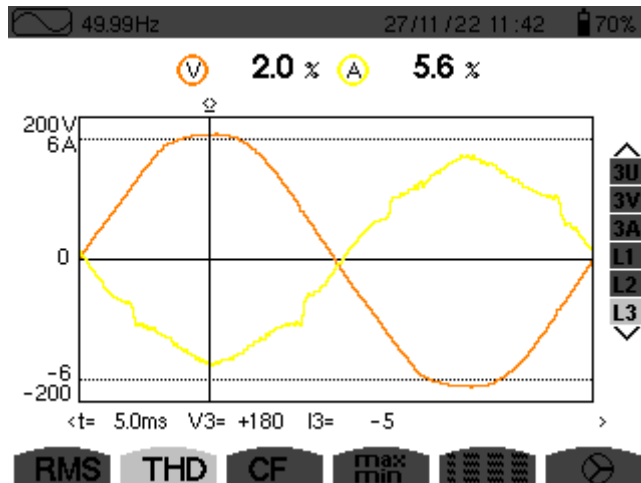

Figure 14. Waveforms of the phase A voltage (orange track) and current (yellow track) while the injection network is active.

Fig. 15 shows voltage and current waveforms at phase 1, accompanied by the corresponding current of the main inverter. Comparing Figs. 15 and 4, it can be seen that waveforms are very similar, and that the inverter current does not flow during the same intervals as in the non-injection case. The inverter output current is increased by the current originating from the current injection network, resulting in the peak current higher than I_{dc}, being equal to 1.75 I_{dc}, but having the same mean of the absolute value.

This means that the switches have to be dimensioned for higher peak currents, but the conduction losses remain the same.
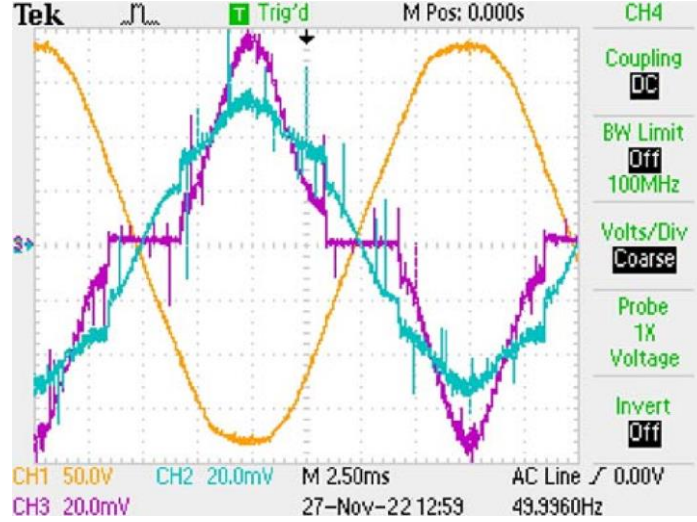

Fig. 15. Waveforms of the phase A voltage (yellow track), current (blue track), and the main inverter current (purple track) when the injection network is active.

In order to analyze the converter efficiency, an issue of interest is to track the power as it flows from the source to the line. It is possible to distinguish two paths: the path through the main inverter, and the path through the current injection device. Similarly, the power taken from the source can be transferred by the buck converter or by the half bridge inverter.

Since the currents through the current injection device contain only the third harmonic, there is no power transfer to the line, because the line voltages do not contain significant harmonic components except the fundamental component. Thus, all the power is transferred through the main inverter.

Regarding the power generation, the current source I_{dc} represents one path of the power transfer from the source. The power transferred here is [12]

$$P_{DC} = V_{OUT,AVG} I_{dc} = \frac{3\sqrt{3}}{\pi} V_m I_{dc}.$$
(9)

The current injection network provides power from the DC link

$$P_{HB} = V_{THB,SEK(3h)}\, I_y = \frac{9\sqrt{3}}{32\pi} V_m I_{dc},$$
(10)

where $V_{THB,SEK(3h)}$ is the RMS value of the third harmonic voltage component at secondary terminals of T_{HB} and $I_{THB,SEK}$ is the RMS value of i_y. Finally, the power taken from the voltage source is

$$P_g = P_{out} = \frac{3\sqrt{3}}{\pi}\left(1 + \frac{3}{32}\right)V_m I_{dc} \tag{11}$$

which means that the buck converter transfers 91.43% of the power, while the half-bridge inverter processes 8.57% of the total power.

It is interesting to compare the theoretical results to the experiment. In the case the injection circuit is not active (Fig. 12), it can be concluded that the amplitude of the phase voltage V_m is equal to 181 V and that the I_{dc} value is approximately 4.15 A. Thus, relation (9) shows that the buck converter output power is 1252 W. Measurement shows that DC voltage at the input terminals of the main inverter is equal to 302.5 V, meaning that the power transferred from buck is equal to 1255.5 W.

Measurement of the power transferred to the line results in 1225 W, meaning that the losses in the main inverter are 30.5 W, which corresponds to 3.7 V voltage drop on the series connection of the IGBT and the diode that form the switch. At the same time, the power taken from the DC source is 1308 W, resulting in 52.5 W of losses in the buck converter, corresponding to the buck converter efficiency of 96%. Total efficiency at 1308 W of the input power and 1225 W of the output power is 93.65%.

In the case the injection system is active, the increase in power is expected to be 116.5 W, meaning that the expected output power is 1359 W. Measurements show that the output power is equal to 1346 W in this case. The buck converter provides 91% of the power, while the injection circuit brings another 9% of the output power. These numbers are very close to theoretical values of 91.43% and 8.57%. The power taken from the DC source than is 1513.5 W. Since the raise in the input power is directed only to the half-bridge inverter, the increase of the input power of 205.5 W and the output power of 121 W results in the injection circuit efficiency of only 59%. Thorough analysis has shown that resistive losses in the injection circuit are 23 W, and that dissipation in the switching circuit is 61.5 W. This is caused by non-optimal turns ratio of the transformer in half-bridge inverter and the high switching frequency, equal to 20 kHz, applied in it to reduce the current ripple. In the case of the optimal turns ratio of the transformer, it would be possible to increase the overall efficiency of the inverter system to about 91.9%.

7. Conclusion

This paper presents a new three-phase voltage-synchronized current source (VSCS) inverter suitable for application in renewable power sources. The inverter uses six unidirectional switches and the third harmonic current

injection circuit. It is shown that it is possible to improve the harmonic content of the line currents and to achieve very low total harmonic distortion, in order of several percent. The output current THD of 6% is experimentally demonstrated, being close to the theoretical minimum of 5,125%. High level of agreement between the theory and the experiments is obtained. Further improvement is possible by optimizing injected current waveform.

Analyzing the power flow and losses, it is shown that all of the power is transferred through the main inverter. Large part of the output power is supplied by the buck converter, while only 9% of the output power is provided by the active part of the current injection network. Further improvements are possible using advanced components.

References

[1]   F. Blaabjerg, Y. Yang, D. Yang and X. Wang, "Distributed powergeneration systems and protection," *Proc. IEEE*, vol. 105, no. 7, pp. 1311-1331, July 2017.

[2]   M. P. Kazmierkowski and L. Malesani, "Current control techniques for three-phase voltage-source PWM converters: a survey," *IEEE Trans. Ind. Electron.*, vol. 45, no. 5, pp. 691-703, Oct. 1998.

[3]   B. Wen, D. Boroyevich, R. Burgos, P. Mattavelli and Z. Shen, "Analysis of d-q small-signal impedance of grid-tied inverters," *IEEE Trans. Power Electron.*, vol. 31, no. 1, pp. 675-687, Jan. 2016.

[4]   L. Harnefors, M. Hinkkanen, U. Riaz, F. M. M. Rahman and L. Zhang, "Robust analytic design of power-synchronization control", *IEEE Trans. Ind. Electron.*, vol. 66, no. 8, pp. 5810-5819, Aug. 2019.

[5]   F.Blaabjerg, Z.Chen, S.B.Kjaer "Power Electronics as Efficient Interface in Dispersed Power Generation Systems", *IEEE Trans. on Power Electronics,* Vol.19, No.5, September 2004.

[6]   [6] R. Strzelecki, G. Benysek "Power Electronics in Smart Electrical Energy Networks ", Springer-Verlag 2008, ISBN 9781848003170

[7]   J.Dai, D.Xu, B.Wu "A Novel Control Systems for Current Source Converter Based Variable Speed PM wind Power Generators", *IEEE Power Electronics Specialists Conference,* pp. 1582-1587

[8]   F.Blaabjerg, Z.Chen "Power Electronics for Modern Wind Turbines", Synthesis Lectures on Power Electronics #1, Morgan & Claypool Publishers, ISBN 1598290320, 2006.

[9] N. Mohan, M. Rastogi, R. Naik, "Analysis of a New Power Electronics Interface with Approximately Sinusoidal 3-Phase Utility Currents and a Regulated DC Output", *IEEE Trans on Power Delivery,* Vol. 8, No. 2, April 1993, pp. 540-546.

[10] P. Pejović, Ž. Janda, "An Analysis of Three-Phase Low-Harmonic Rectifiers Applying the Third-Harmonic Current Injection", *IEEE Transactions on Power Electronics*, Vol. 14, No. 3, May 1999, pp. 397-407.

[11] P. Pejović, Ž. Janda ,"An Improved Current Injection Network for Three-Phase High-Power-Factor Rectifiers that Apply the Third Harmonic Current Injection", Letters to the Editor in IEEE Transactions on Industrial Electronics, Vol. 47, No. 2, April 2000, pp. 497-499

[12] Ž. Janda, P. Pejović, P. Ninković,"Nova topologija strujnog invertora povišene efikasnosti za obnovljive izvore električne energije", *14. International Symposium on Power Electronics*, Ee 2007, Novi Sad.

[13] Power Electronics: Converters, Applications And Design, N. Mohan, T.M. Undeland, W.P. Robbins, John Wiley & Sons. 2002

Acknowledgement

Kratak sadržaj: U radu se predlaže nova topologija trofaznog strujnog invertora čiji prekidači rade u sinhronizmu sa trofaznim mrežnim naponom i koristi se tehniku ubrizgavanja trećeg harmonika. U poređenju sa konvencionalnom vektorskom kontrolom struje, ova metoda potpuno uklanja potrebu za fazno-zaključanim petljama a time i dodatnu dinamiku. Ovaj novi tip strujnog pretvarača sinhronog sa mrežnim naponom je pogodan za primenu u mrežno povezanim obnovljivim izvorima energije. Zasnovan je na topologiji trofaznog šestoimpulsnog invertora sa unidirekcionim prekidačima i sinhronoj kontroli prekidača za postizanje jediničnog faktora snage na mestu priključenja na mrežu. Dodatni pretvarač za implementaciju tehnike ubrizgavanja trećeg harmonika struje se koristi kako bi se poboljšalo ukupno izobličenje struje koja teče prema mreži. Predložena obezbeđuje stabilan rad u uslovima slabe mreže. Prikazani su I diskutovani eksperimentalni rezultati dobijeni testiranjem prototipa od 1,5 kW sa optimalnim ubrizgavanjem trećeg harmonika struje. Teorijska predviđanja poboljšanja ukupnog izobličenja mrežne struje i faktora snage su eksperimentalno potvrđena.

Trofazni strujni invertor sa ubrizgavanjem trećeg harmonika za obnovljive izvore energije povezane na mrežu

Predrag Ninković, Žarko Janda, Predrag Pejović